THE JOURNAL OF PHYSICAL CHEMISTRY C
A JOURNAL OF THE AMERICAN CHEMICAL SOCIETY

pubs.acs.org/JPCC

Article

Thermal Decomposition of Dimethyl Methylphosphonate on Size-Selected Clusters: A Comparative Study between Copper Metal and Cupric Oxide Clusters

Published as part of The Journal of Physical Chemistry virtual special issue "Daniel Neumark Festschrift".

Linjie Wang, Michael Denchy, Nicolas Blando, Lucas Hansen, Ben Bilik, Xin Tang, Zachary Hicks, and Kit H. Bowen*

Cite This: *J. Phys. Chem. C* 2021, 125, 11348–11358

Read Online

ACCESS | Metrics & More | Article Recommendations | Supporting Information

ABSTRACT: Room temperature decomposition and thermal decomposition of dimethyl methylphosphonate (DMMP), a chemical warfare agent (CWA) simulant, on size-selected copper clusters have been studied via combined X-ray photoelectron spectroscopy (XPS) and temperature-programmed desorption (TPD). Cu_{100} and $(CuO)_{80}$, which have the same nominal masses, were chosen to present a direct comparison between the reactivity of metallic copper and that of cupric oxide with DMMP. Room temperature XPS results have shown that most of the DMMP molecules decompose completely and reductively into atomic phosphorus on Cu_{100}, while almost all the DMMP molecules are only dissociatively adsorbed on $(CuO)_{80}$ as methyl methylphosphonate (MMP). XPS and TPD have been carried out to analyze the thermal decomposition of adsorbed DMMP by identifying the surface species after annealing to certain temperatures and the gaseous products evolved during linear temperature ramps, respectively. Methanol, formaldehyde, and methane are the three most significant gaseous products for DMMP decomposition on both Cu_{100} and $(CuO)_{80}$. Methanol and formaldehyde, which evolve in the low temperature region, are believed to originate from surface methoxy species. Methanol, formaldehyde, and methane evolved in the high temperature region are related to further decomposition of the phosphorus-containing surface species. A set of methanol-probed TPD experiments have also been carried out, which suggest that methane evolution originates from the methyl group within DMMP instead of the surface methoxy species.

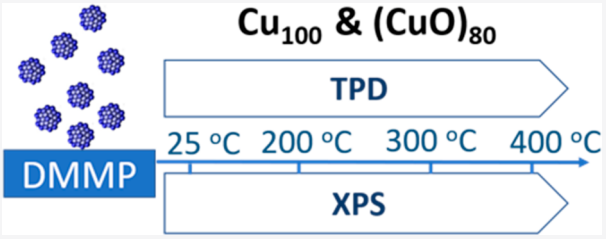

INTRODUCTION

Synthetic organophosphonates are ubiquitous in the agricultural, chemical, and pharmaceutical industries.[1] One group of organophosphonates, which are especially notorious, is chemical warfare agents (CWAs).[2] Dimethyl methylphosphonate (DMMP) is a commonly used simulant for one of those highly toxic CWAs, i.e., sarin, and it has been used extensively during the development of sensors and the study of catalytic decomposition processes.[3,4] DMMP and many other similar pesticide molecules are also studied in the field of environmental chemistry.[5−7] Due to high perseverance, toxicity, and potential for bioaccumulation, their removal is imperative.[8] To this end, developing a more fundamental understanding of how DMMP decomposes on different surfaces is highly imperative.

The adsorption and decomposition chemistries of DMMP have been studied on an extensive library of metal oxide surfaces, such as Al_2O_3,[9−12] SiO_2,[13−15] TiO_2,[16−23] CeO_2,[24−26] WO_3,[19,27] MoO_2,[28] MoO_3,[29−31] Fe_2O_3,[12,16,24] CuO,[32] Cu_2O,[33] and so on. On most of these metal oxide surfaces, DMMP first adsorbs via its phosphoryl oxygen (P═O) at the coordinatively unsaturated metal ion sites or on surface hydroxyls at relatively low temperature (typically below room temperature).[4,14,16,19,23,28] The P═O bond can convert to a bridging O−P−O moiety at near room temperature.[23,26] Adsorbed DMMP can then undergo stepwise elimination of methoxy groups upon heating.[11,19,22] The formation of methyl methylphosphonate (MMP) and surface methoxy species via P−OCH_3 bond scission is commonly seen as the first decomposition step on many metal oxides.[9,19,22,28] The P−CH_3 bond usually stays intact before scission of the two P−OCH_3 bonds within one DMMP molecule.[19] However, exceptions have been reported for DMMP decomposition on CuO and Cu_2O surfaces, both of which have shown room temperature P−CH_3 scission.[32,33] The evidence that a small

Received: February 1, 2021
Revised: May 6, 2021
Published: May 19, 2021

https://doi.org/10.1021/acs.jpcc.1c00952
J. Phys. Chem. C 2021, 125, 11348−11358

portion of adsorbed DMMP can decompose completely into atomic phosphorus on Cu_2O,[33] but not on CuO,[32] suggests that the oxidation states of metal ions in metal oxide materials can have significant effects on their reactivity toward DMMP.

Besides metal oxides, DMMP adsorption and decomposition studies have also been done on single crystal surfaces, such as Ni(111),[34] Pd(111),[34] Pt(111),[35] Rh(111),[36] and Mo(111).[37] Metallic copper has been investigated in the form of copper clusters and films supported on TiO_2(110),[38] as well as Cu/TiO_2 composite aerogels.[39] However, the sample preparation procedures in these two studies may have produced a copper oxide layer on top of the metallic copper. As a result, these two studies have shown some similarities to the work done on pure CuO, Cu_2O, and TiO_2 surfaces. Considering the fact that copper oxide surfaces have shown unique reactivities toward DMMP, while the actual reactivity of metallic copper remains unclear, a direct comparative study between metallic copper and copper oxide is desirable.

Ultrasmall clusters, which have high surface-to-volume ratios and a high percentage of low-coordinated metal atoms on the surface, have unique physical and chemical properties that are distinct from their macroscopic counterparts. Numerous studies have highlighted the ability of the cluster deposition method to explore the reactivity of ultrasmall clusters, with different sizes and composition, supported on a given substrate.[40] In this work, Cu_{100} and $(CuO)_{80}$ clusters were size-selected and deposited onto a highly oriented pyrolytic graphite (HOPG) substrate, where they were exposed to DMMP. Combined X-ray photoelectron spectroscopy (XPS) and temperature-programmed desorption (TPD) characterizations were carried out to analyze the room temperature decomposition and thermal decomposition of DMMP, respectively. Based on this direct comparison between metallic copper and cupric oxide in cluster forms, the rather significant effect that the metal oxidation state within the clusters can have on their reactivity toward DMMP is demonstrated and the unique reactivity of Cu_{100} is highlighted.

EXPERIMENTAL SECTION

Formation and Deposition of Clusters. Copper and copper oxide cluster anions were generated in a magnetron sputtering source. After acceleration, mass selection and deceleration, the clusters were then deposited (soft-landed, < 1 eV/atom) onto an HOPG substrate (Bucker, ZYB grade, 12·12 mm^2, 2 mm thickness) under ultrahigh vacuum (UHV, base pressure 5×10^{-9} Torr).

In the magnetron sputtering source, a copper sputtering target (Kurt J. Lesker Co, 99.99%) was placed in front of a circular magnet and biased by up to −500 V, where a mixture of argon (Airgas, 99.999%) and helium (Airgas, 99.999%) with a ratio of 1:1−1.2 (Ar/He) was introduced. Argon gas was ionized to create argon cations, which sputtered the metal target to produce a plasma. Helium served to cool and transport the cluster anions down the beamline. Anionic clusters were first electrostatically accelerated to 500 eV and then entered a magnetic sector mass filter (25° sector magnet with resolution of $m/\Delta m = 20$). By tuning the magnetic field strength, a beam of Cu_n^- cluster anions of the desired size was mass-selected. The size-selected cluster anions were then deflected and focused into the deposition chamber, where they were decelerated and finally soft-landed onto the HOPG substrate. $(CuO)_n^-$ clusters were generated, transported, and deposited in the same manner, with the addition of oxygen into the Ar/He mixture via a dosing valve (INFICON VDH016-x) with an oxygen (Airgas, 99.994%) backing pressure of 15 psi. By reducing the dosing to a negligible pressure and lowering the oxygen backing pressure to 5 psi, $(CuO_{1-x})_n^-$ clusters were generated for comparative experiments. Cu_n^- ($n = 100 \pm 5$), $(CuO)_n^-$ ($n = 100 \pm 4$), and $(CuO_{1-x})_n^-$, which all have the same atomic mass range, were selected via the magnetic sector with the same settings. Once deposited on the surface, the anionic clusters lost their negative charges to form neutral species. For the convenience of expression, Cu_{100}, $(CuO)_{80}$, and $(CuO_{1-x})_n$ are used in the rest of this article to denote these three groups of clusters with the same confined mass range.

During a deposition process, the deposition current was monitored by a picoammeter, and the coverage of the as-deposited clusters was given in current (ampere, A) integrated over time (second, s). For each deposition, the average deposition current was about 70 pA, corresponding to an average flux of 4×10^8 clusters per second; and the final deposition amount was controlled to be 1×10^{-6} A·s, corresponding to a total amount of 6×10^{12} clusters.

Temperature-Programmed Desorption (TPD). TPD experiments were carried out via the liquid nitrogen matrix deposition (LNMD) method. This method was originally inspired by the common experimental technique used in matrix isolation infrared spectroscopy.[41] It was then adopted to probe the activities of metals or metal oxides toward a reactive matrix.[42] In our lab, the LNMD method was successfully implemented in order to probe the ligation and decomposition process of 1,6-hexanedithiol on size-selected Cu_{100} clusters.[43]

Prior to cluster deposition, the HOPG substrate was cleaved under ambient conditions right before being transported into a load-lock chamber and then into a UHV chamber. The substrate was then annealed at 500 °C for 30 min. This preparation step was proven to be adequate to obtain a relatively low background in a control TPD run, in which no clusters were deposited while all the other experimental conditions remained the same. The as-prepared HOPG was then cooled and maintained at −170 °C by a liquid nitrogen reservoir. DMMP (Sigma-Aldrich, 97%) was degassed and purified by three freeze−pump−thaw cycles before being dosed into the vacuum chamber through a UHV compatible leak valve. The dose of DMMP was monitored by a pressure gauge and a residual gas analyzer (RGA) (Hiden HAL/3F PIC quadrupole mass spectrometer (QMS)). The dose amount was 1×10^{-8} Torr for 100 s, i.e., 1 Langmuir (L, 10^{-6} Torr·s), which was sufficient to form a frozen multilayer matrix of DMMP on HOPG at −170 °C. After dosing, size-selected clusters were deposited into the premade frozen DMMP matrix.

After cluster deposition, the sample was ramped from −170 to +25 °C by resistive heating to remove the physi-adsorbed DMMP. Once warmed up to 25 °C, DMMP had likely been irreversibly adsorbed by the clusters, while most unreacted DMMP had already been physi-desorbed. TPD was then carried out to characterize the thermal decomposition properties of DMMP on the size-selected clusters. The gaseous decomposition products were detected and identified via a residual gas analyzer (RGA), which was positioned normal to the plane of the substrate at a distance of about 5 mm. Moreover, the entrance of the RGA is covered by a glass shroud with a 6 mm diameter hole cut at the center. These two configurations can both help to minimize the contributions

https://doi.org/10.1021/acs.jpcc.1c00952
J. Phys. Chem. C 2021, 125, 11348−11358

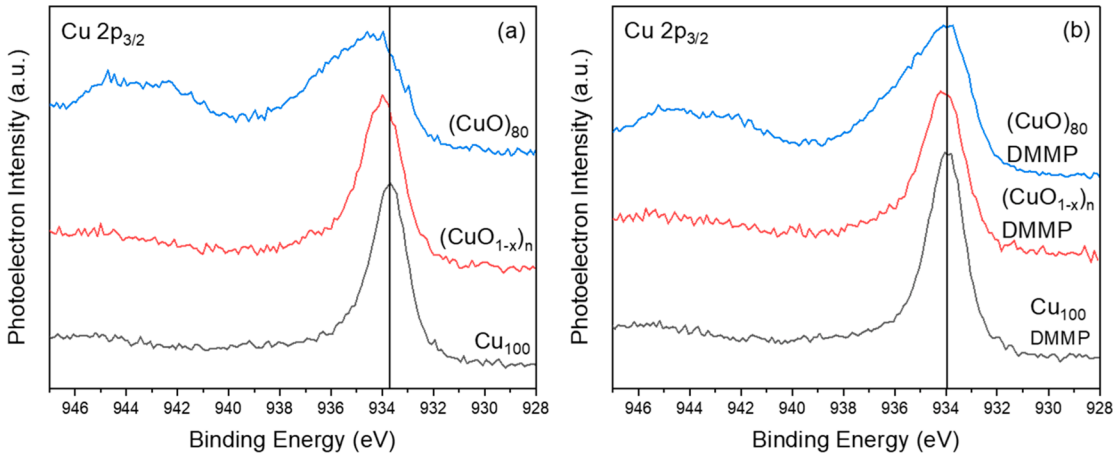

Figure 1. Cu $2p_{3/2}$ XPS on bare clusters and DMMP-adsorbed clusters. (a) Cu $2p_{3/2}$ XPS on bare $(CuO)_{80}$ (blue), $(CuO_{1-x})_n$ (red), and Cu_{100} (black). (b) Cu $2p_{3/2}$ XPS on DMMP absorbed $(CuO)_{80}$ (blue), $(CuO_{1-x})_n$ (red), and Cu_{100} (black).

from background gases and to maximize the sensitivity toward the species desorbing directly from the substrate. Regarding the customized TPD sample holder, two small pieces of tantalum foil are wrapped on two copper power feedthroughs to allow for resistive heating, where the HOPG substrate is held. A k-type thermocouple joint is spring-loaded to the back of the HOPG for temperature measurement and to ensure a linear heating ramp.

X-ray Photoelectron Spectroscopy (XPS). The method by which DMMP binds and decomposes on copper and copper oxide clusters was characterized via XPS with nonmonochromatic Mg Kα rays (1253.6 eV), and a hemispherical analyzer (PerkinElmer PHI 5100 10−360). For XPS measurements at varied temperatures, the sample was heated to certain critical temperatures and then cooled back down to room temperature, at which point XPS spectra were acquired. All the XPS spectra were calibrated by graphite C 1s at 284.5 eV.[44]

The cluster source, beamline, cluster deposition, and surface instrumentation are all within one vacuum system separated by gate valves. The sample can be transferred between two vertical manipulators by a horizontal magnetic transfer arm. More details about this apparatus are described elsewhere.[45]

RESULTS

Room Temperature XPS Characterization. XPS measurements were carried out at room temperature on bare clusters as well as DMMP-adsorbed clusters to elucidate how DMMP reacts differently between copper and copper oxide clusters. Figure 1a shows Cu $2p_{3/2}$ XPS spectra for the bare clusters. Specifically, the spectrum for $(CuO)_{80}$ has a broad main peak at around 934.2 eV and a strong satellite feature in the range of 940−950 eV, which confirms that the majority of the Cu atoms should be in the Cu^{2+} oxidation state. Whether or not a small amount of Cu^0 or Cu^{1+} also exists is not clear based on the Cu $2p_{3/2}$ XPS spectrum alone. By contrast, the spectrum for Cu_{100} has a much narrower peak with a lower binding energy at around 933.7 eV, indicating a Cu^0 or Cu^{1+} oxidation state. Moreover, the spectrum in the middle, which has no obvious satellite peak, confirms no evident existence of a Cu^{2+} oxidation state above the detection limit. Additionally, the black vertical line in Figure 1a, which marks the approximate peak positions for Cu_{100}, indicates that the clusters corresponding to the middle spectrum may have an intermediate oxidation state between those that have been observed for (CuO_{80}) and Cu_{100}, respectively. This argument is made not solely based on the Cu 2p spectrum but also with consideration of the clusters synthesis procedures as well as the P 2p spectra, which are discussed later on. Since there is no further evidence on whether or not the clusters exhibit purely Cu^{1+} or a mixture of different oxidation states, it is therefore denoted as $(CuO_{1-x})_n$ in this work.

How DMMP reacts differently among these three clusters with varied copper oxidation states is shown by comparing part b to part a of Figure 1 for each cluster. First, the spectrum for DMMP-adsorbed $(CuO)_{80}$ in Figure 1b shows a slightly narrower main peak and a weaker satellite feature compared to the one in Figure 1a, implying partial reduction of Cu^{2+} to Cu^{1+}. The possibility of Cu^{2+} reduction cannot be excluded here as it was done by Trotochaud et al.[32] due to low signal-to-noise ratio and lack of other characterization methods. Second, for DMMP-adsorbed $(CuO_{1-x})_n$, there is no obvious binding energy shift for Cu $2p_{3/2}$ relative to the bare cluster. Third, for DMMP-adsorbed Cu_{100}, the Cu $2p_{3/2}$ peak shifts to a slightly higher binding energy, suggesting an oxidative effect of DMMP on the copper metal clusters as compared to the copper oxide clusters. Furthermore, the two vertical lines, which mark the approximate peak positions for Cu_{100} in parts a and b of Figure 1, show that the binding energy trends are different before and after DMMP adsorption. It is clearly shown that the Cu $2p_{3/2}$ binding energies from Cu_{100} to $(CuO)_{80}$ bare clusters exhibit an increasing trend (Figure 1a). However, this increasing trend is apparently weakened for DMMP-adsorbed clusters, possibly due to oxidative effects that DMMP may have on metallic copper clusters, as well as reductive effects that DMMP may have on cupric oxide clusters. In brief, as a result of DMMP adsorption, the binding energies of Cu $2p_{3/2}$ from these three clusters become much closer to each other. However, based on Cu $2p_{3/2}$ XPS spectra alone, no further conclusions can be drawn.

Other than Cu $2p_{3/2}$ XPS, P 2p XPS measurements of DMMP absorbed clusters can give further evidence as to how DMMP reacts differently between Cu_{100} and $(CuO)_{80}$, with $(CuO_{1-x})_n$ representing an intermediately oxidized state. As is shown in Figure 2a−c, the three P 2p spectra contain two main groups of phosphorus species marked by two vertical lines. The one with higher binding energy, centered at around 133.5 eV, is assigned to adsorbed phosphonate species. The other one,

https://doi.org/10.1021/acs.jpcc.1c00952
J. Phys. Chem. C 2021, 125, 11348−11358

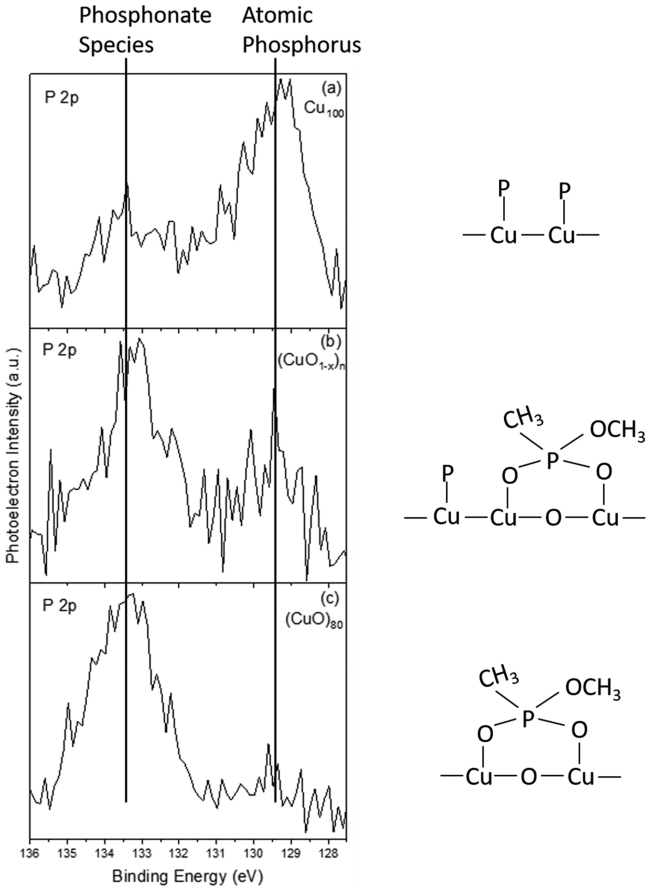

Figure 2. P 2p XPS on DMMP-adsorbed clusters: (a) Cu_{100}, (b) $(CuO_{1-x})_n$, and (c) $(CuO)_{80}$. The two vertical lines mark the two main groups of phosphorus-containing species, which are phosphonate species and atomic phosphorus. The corresponding diagrams are shown on the left for each cluster.

with a binding energy below 130 eV, is assigned to adsorbed atomic phosphorus. As is shown in Figure 2a, the phosphorus species on Cu_{100} are almost exclusively atomic phosphorus with only a very small amount of phosphonate species. In this sense, most of the DMMP molecules adsorbed on Cu_{100} have decomposed completely. By contrast, there is no obvious signal for any atomic phosphorus on $(CuO)_{80}$ (Figure 2c). Instead, DMMP mainly undergoes cleavage of one P−OCH_3 bond and forms adsorbed methoxy and methyl methylphosphonate (MMP), which is a partial decomposition process. For $(CuO_{1-x})_n$, which has an intermediate copper oxidation state, an intermediate state is also observed in P 2p XPS measurements. As is shown in Figure 2b, $(CuO_{1-x})_n$ has a fair amount of both adsorbed phosphonate species and atomic phosphorus, with the phosphonate species as the dominant adsorbate. In brief, room temperature XPS measurements have shown that Cu_{100} can lead to the complete breakdown of DMMP into atomic phosphorus while $(CuO)_{80}$ can only cause partial dissociation of DMMP into adsorbed phosphonate species.

XPS Characterization after Heating to Certain Temperatures. It is known that DMMP can undergo further decomposition at elevated temperature. Therefore, XPS spectra, which were collected after heating the sample to certain temperatures and then cooling back down to room temperature, are shown here to compare the thermal decomposition processes of DMMP on Cu_{100}, and $(CuO)_{80}$.

For the Cu $2p_{3/2}$ spectra, after heating to 200 °C or beyond, there is no obvious change in either peak position or peak shape (Figure 3a). For $(CuO)_{80}$, the major change only occurs when annealed to 200 °C (Figure 3b). The facts that the satellite features disappear and that the main peak becomes narrower and shifts to a lower binding energy indicate the reduction of the majority of Cu^{2+} to Cu^{1+}. Similarly, there is no obvious change after annealing to 300 and 400 °C.

For the P 2p spectra, the major difference between Cu_{100} and $(CuO)_{80}$ remains in the low binding energy region from 128 to 131 eV. As is shown in Figure 3c, the vertical line marks the low binding energy area, which is mainly atomic phosphorus on Cu_{100} for all four annealing temperatures. By contrast, there is no obvious atomic phosphorus peak for $(CuO)_{80}$ (Figure 3d). As for the high binding energy region from 131 to 135 eV, the P 2p peaks for both Cu_{100} and $(CuO)_{80}$ share a similar trend with incremented temperatures, despite a great difference in peak intensity. As is shown in Figure 3, parts c and d, the two diagonal lines mark the two similar rising binding energy trends with incremented temperatures. Because of the abundance of phosphonate species on $(CuO)_{80}$, it is clearly shown that the major binding energy shift happens upon heating to 200 °C. After heating to 300 °C, there is no obvious change in the peak position. Even so, given that the peak position shifted to the highest binding energy for 400 °C, the overall trend in binding energy shift is still an increase with incremented temperatures. Similarly, the weak phosphonate peaks for Cu_{100} also shift to higher binding energies after annealing (Figure 3c).

In short, XPS measurements after heating to certain temperatures have shown that atomic phosphorus formed due to complete decomposition of DMMP is only observed for Cu_{100} and that phosphonate species formed due to partial dissociation of DMMP are observed to a large extent on $(CuO)_{80}$ and only to a minor extent on Cu_{100} at room temperature, with further decomposition observed at elevated temperatures.

Temperature-Programmed Desorption (TPD). The gaseous products formed during the thermal decomposition processes of DMMP on Cu_{100} and $(CuO)_{80}$ clusters were studied via TPD. Several DMMP fragments and likely reaction products were monitored. The three major products are plotted in Figure 4 after being corrected for fragmentation. More details on the correction process are described in the Supporting Information.

As is shown in parts a and b of Figure 4, methanol, formaldehyde and methane are the three major gaseous products for both Cu_{100} and $(CuO)_{80}$. There are apparently two desorption regions: the low temperature region from 120 to 220 °C and the high temperature region from 220 to 320 °C. For Cu_{100}, the methanol spectrum has a rising shoulder feature culminating in a peak, which coincides with formaldehyde in the low temperature region. In the high temperature region, methane evolves at a slightly lower temperature than that of the second peak of formaldehyde. For $(CuO)_{80}$, the peaks of all three products occur in the high temperature region, with methanol and formaldehyde having rising shoulder features in the low temperature region. By comparison, both Cu_{100} and $(CuO)_{80}$ have a methane peak and a formaldehyde peak in the high temperature region, while the major differences lie in the low temperature region, where

https://doi.org/10.1021/acs.jpcc.1c00952
J. Phys. Chem. C 2021, 125, 11348−11358

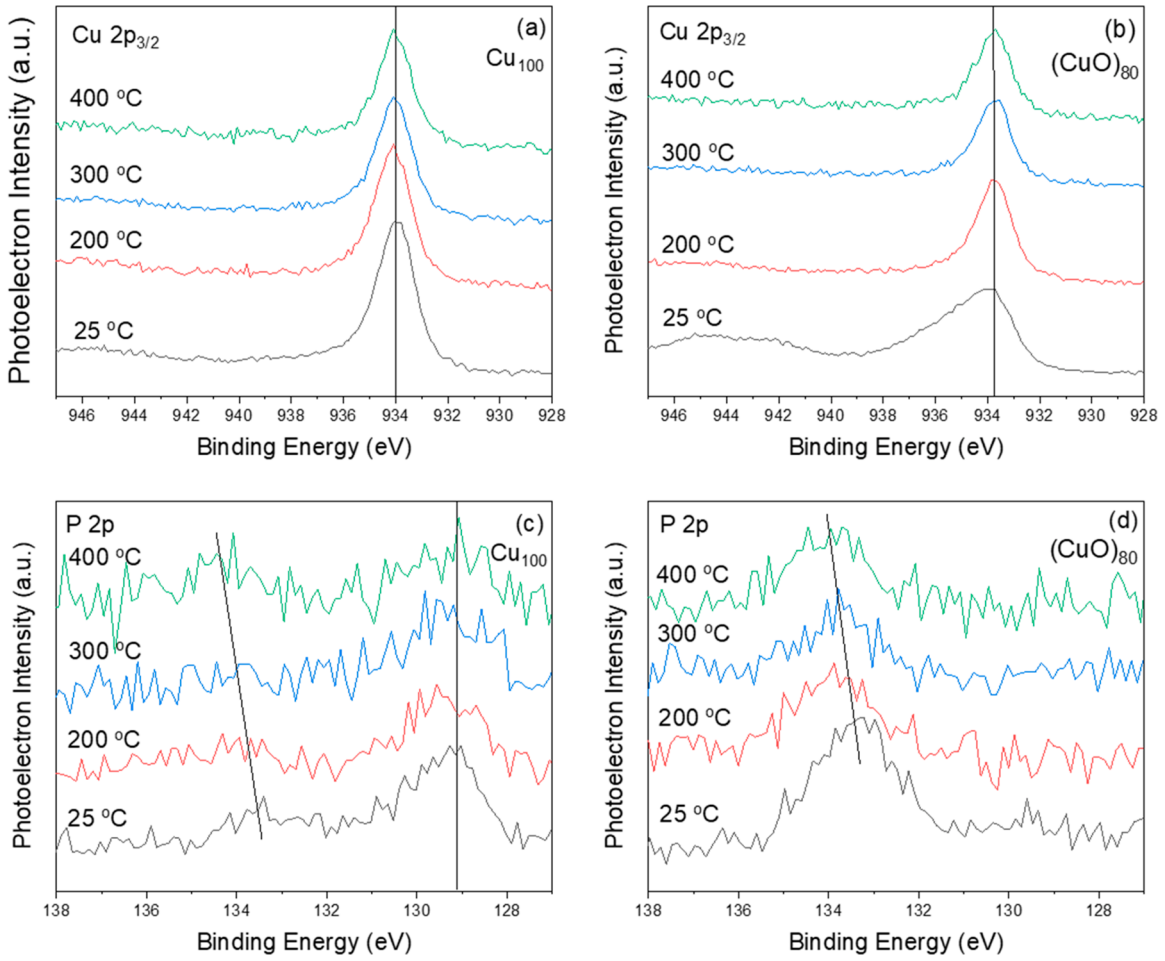

Figure 3. XPS of Cu $2p_{3/2}$ and P 2p for DMMP-adsorbed Cu_{100} and $(CuO)_{80}$ clusters at 25 °C and after heating to 200, 300, and 400 °C: (a) Cu $2p_{3/2}$ XPS for DMMP-adsorbed Cu_{100}; (b) Cu $2p_{3/2}$ XPS for DMMP-adsorbed $(CuO)_{80}$; (c) P 2p XPS for DMMP-adsorbed Cu_{100}; (d) P 2p XPS for DMMP-adsorbed $(CuO)_{80}$. For all four graphs, spectra are presented from bottom to top in order of increasing temperature, which are color coded as 25 (black), 200 (red), 300 (blue), and 400 °C (green). Vertical and diagonal lines in all the graphs, which mark the approximate peak positions, show the binding energy shifting trends with incremented temperatures.

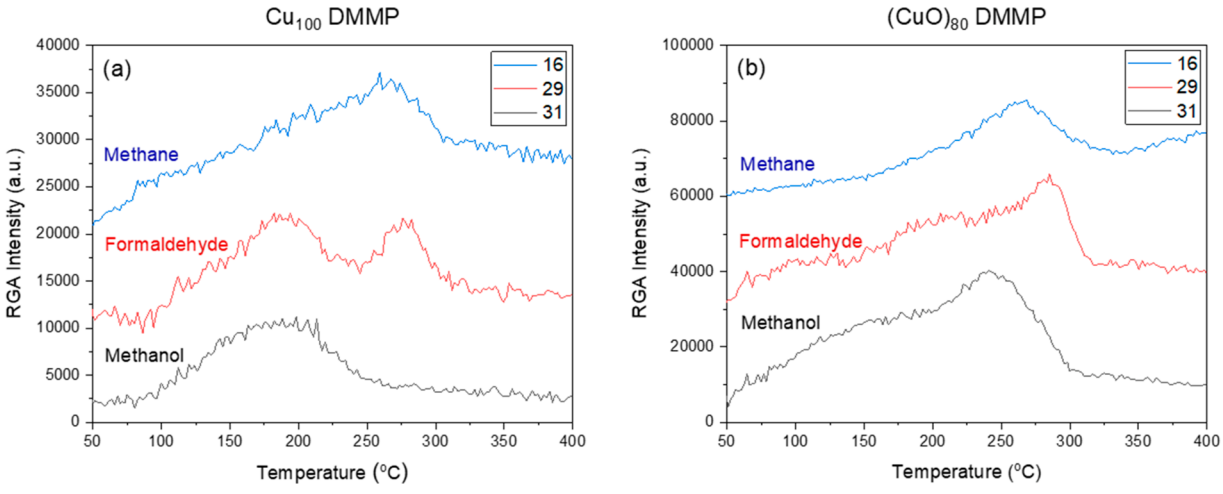

Figure 4. DMMP decomposes into methanol (black), formaldehyde (red), and methane (blue) on Cu_{100} and $(CuO)_{80}$ in TPD experiments. Methanol, formaldehyde, and methane are tracked by m/e of 31, 29 and 16, respectively. The traces are offset for clarity, and data have been corrected for fragmentation patterns.

Cu_{100} has a significant peak for both formaldehyde and methanol but $(CuO)_{80}$ only has broad shoulder features for each species.

https://doi.org/10.1021/acs.jpcc.1c00952
J. Phys. Chem. C 2021, 125, 11348−11358

DISCUSSION

The results presented here demonstrate the unique reactivity of Cu_{100} with DMMP at room temperature when compared to that of $(CuO)_{80}$. Specifically, the fact that DMMP mainly decomposes into atomic phosphorus on Cu_{100} at room temperature is quite exceptional. At elevated temperatures, XPS and TPD offer greater details on the thermal decomposition process of DMMP on Cu_{100} and $(CuO)_{80}$. Here, we will start our discussion with the assignment of features in the XPS spectra and its limitations in identifying surface species in this study. Next, a set of methanol-probed TPD experiments will be presented to provide further insights regarding the origin of the gaseous products. Finally, a proposed reaction scheme considering both the XPS and TPD results will be discussed.

Assignment of Features in XPS Spectra. A formal peak fitting process has not been applied to the P 2p spectra due to low signal-to-noise ratio. Since size-selected cluster deposition experiments generally have prepared samples with low cluster coverage, and phosphorus has a low relative sensitivity factor, it is expected that the signal intensity for P 2p XPS should be very low. Therefore, no specific binding energy for phosphorus species has been reported here to avoid overinterpretation of the data. Instead, rational speculations have been drawn for the low (128−130 eV), middle (130−133 eV), and high (133−135 eV) binding energy range. It is generally accepted that phosphorus species with fewer oxygen-containing coordinated groups tend to have lower P 2p binding energies.[46] Accordingly, those phosphorus species, which have no coordinated oxygen, usually have the lowest binding energies. For example, a binding energy of 128.5 eV was reported for atomic phosphorus on copper clusters supported on $TiO_2(110)$.[38] Similarly, the low binding energy peak is assigned as mostly atomic phosphorus on Cu_{100}. Moreover, Lai et al. demonstrated a stepwise dealkylation of PR_3 (R is methyl or ethyl) on Cu(110), showing that PR_3, PR_2, and PR have P 2p binding energies of 131.6, 130.8, and 129.6 eV, respectively.[47] Considering that DMMP only has one methyl group to begin with, even though there is no discernible peak feature in the middle binding energy area, it is speculated that there may be some surface $-PCH_3$. Furthermore, a surface-bound phosphinate group [O═PH(OCH_3)O−Cu] with a binding energy of 132.5 eV was identified for DMMP decomposition on polycrystalline cuprous oxide surfaces at room temperature.[33] Even though there is no discernible feature in the middle binding energy area, it is speculated that there may be an analogous phosphinate group. These arguments are discussed further in the following sections.

DMMP physisorbed on different metal oxides was reported to be in the range of 134.0−135.0 eV, while chemisorbed DMMP was reported to have a slightly lower binding energy.[33] In this work, the binding energy of P 2p for molecular DMMP was also measured in the form of a frozen DMMP matrix on HOPG without any clusters. As is shown in Figure S1, intact DMMP has a binding energy of 134.2 eV, while the peak positions in the high binding energy range shown in parts c and d of Figure 3 are clearly below 134 eV. Methyl methylphosphonate (MMP), which is a dissociative adsorption product of DMMP, was identified on metal oxides with binding energies lying in the range of 132.8−133.8 eV.[31−33] Moreover, extensive IR studies have provided direct evidence for the formation of MMP and surface-adsorbed methoxy groups at or below room temperature on other metal oxide surfaces.[23] Therefore, the peak feature in the high binding energy area at room temperature is assigned to mostly MMP.

Upon heating to 200 °C, there is no obvious change in low and middle binding energy range. In the high binding energy range, the peak position shifts to an even higher binding energy. It is speculated that the decomposition of both phosphinate and MMP may contribute to the formation of PO_x through P−O bond and P−C bond scission, which has been proposed in a study of DMMP decomposition on a Cu_2O surface.[33] Moreover, potential surface-bound $-PCH_3$ is speculated to decompose into atomic phosphorus via P−C bond cleavage upon heating to 200 °C. However, this phenomenon was not observed at all in the work on Cu_2O. In fact, atomic phosphorus disappeared completely on Cu_2O after heating to 160 °C.[33] In this sense, the abundance and accumulation of atomic phosphorus in this work are attributed to the unique reactivities of metallic copper in Cu_{100}.

Once annealed to 300 °C, the two peaks lying within the low and high binding energy range seem to be more ambiguously separated from each other, indicating other types of phosphorus-containing species may have formed in the middle binding energy range. It is speculated that oxidative decomposition of $-PCH_3$ and oxidation of atomic phosphorus can both give rise to the increased signal intensity detected in the middle binding energy range. This may seem contradictory, because $-PCH_3$ is believed to partially decompose into atomic phosphorus after heating to 200 °C, which is a reductive process. A reasonable explanation is that the residual water and oxygen in the chamber can cause oxidation during the heating and cooling processes for XPS experiments, which usually last several hours. The higher the ultimate temperature attained, the longer the experiment has lasted, thus leading to the higher degree of oxidation. This can also explain why the atomic phosphorus peak is further weakened, and the PO_x peak becomes even stronger at 400 °C. It is also reasonable to speculate that the surface phosphorus species lying in the middle binding energy range at 300 °C may undergo further oxidation into PO_x during the heating process from 300 to 400 °C. After annealing to 400 °C, only PO_x and atomic phosphorus are present due to their relatively higher thermodynamic stability.

Unlike Cu_{100}, there is no obvious peak in the low binding energy range for $(CuO)_{80}$. At room temperature, the main peak in the high binding energy range is assigned to MMP, which has also been identified on polycrystalline CuO surfaces.[32] The very weak peak feature in the low binding energy range can be explained by the existence of a small amount of atomic phosphorus or the satellite features for Cu 3s. Recalling the fact that both Cu_{100} clusters and polycrystalline Cu_2O can give rise to complete decomposition of DMMP into atomic phosphorus at room temperature, the presence of a trace amount of atomic phosphorus here indicates that some residual Cu^0 or Cu^{1+} may have played a role within the size-selected $(CuO)_{80}$ clusters. It should be noted that the main peak of a typical Cu 3s spectrum lies in the range of 123.0−124.0 eV and that Cu 3s spectra in Cu^{2+} compounds have satellite features that lie in the range of 3 to 10 eV higher in binding energy relative to the main peak. In this sense, the satellite features of Cu 3s in the $(CuO)_{80}$ Cu 3s spectrum can overlap with the P 2p peak region, especially the low binding energy range for atomic phosphorus. Due to the limitation of

https://doi.org/10.1021/acs.jpcc.1c00952
J. Phys. Chem. C 2021, 125, 11348−11358

Scheme 1. Proposed Reaction Scheme of DMMP Decomposition on Cu_{100} and $(CuO)_{80}$

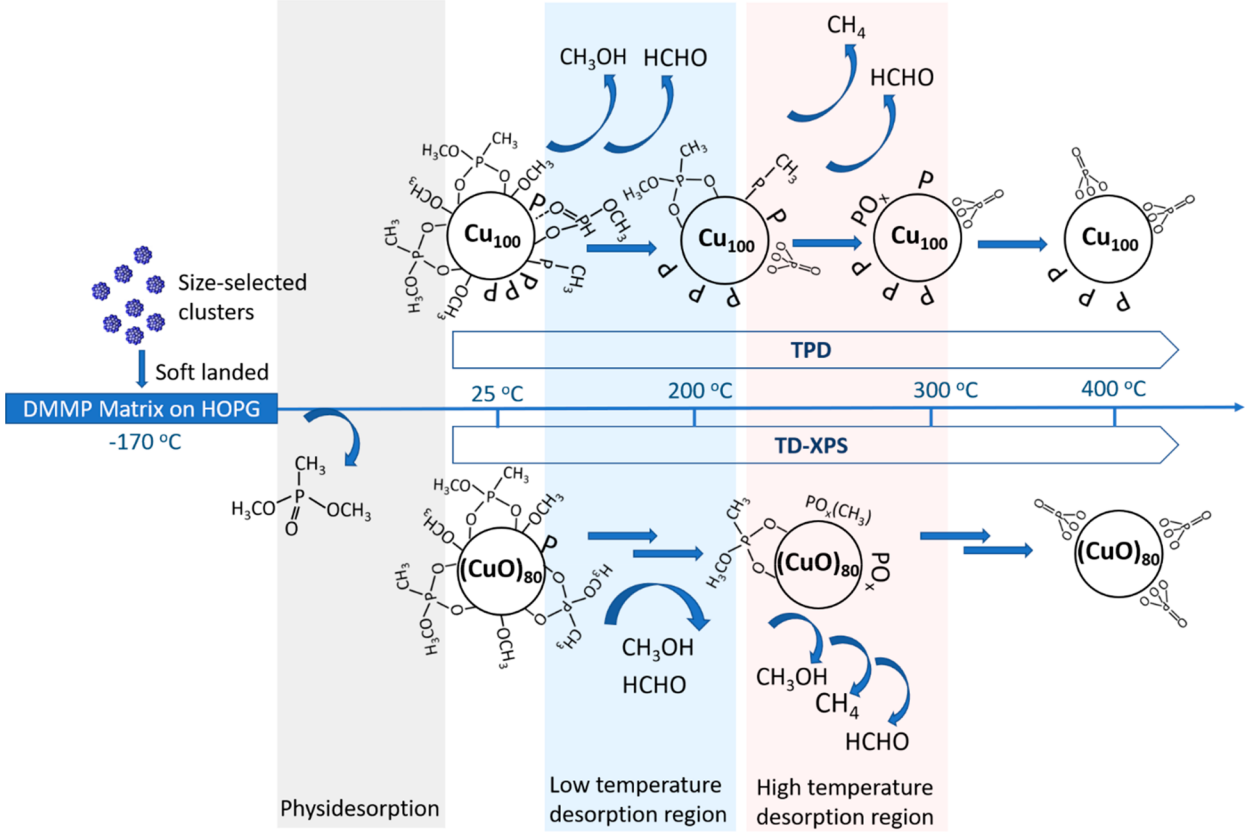

low signal-to-noise ratio, neither of these two explanations can be ruled out.

After heating to 200 °C, it is clearly shown that the low binding energy feature has vanished and the MMP peak has shifted slightly to higher binding energy. It should be mentioned that Cu^{2+} in bare $(CuO)_{80}$ clusters can be reduced completely to Cu^{1+} upon annealing to 200 °C under UHV (Figure 3b). Moreover, multiple studies have shown that lattice oxygen in CuO can participate in dissociative adsorption and oxidative decomposition processes at room temperature and elevated temperatures for many organic molecules such as DMMP,[32] methanol,[48,49] and alkanethiols.[43,50] Therefore, the disappearance of low binding energy feature can be ascribed to the oxidative effects on potential atomic phosphorus from the activated lattice oxygen within $(CuO)_{80}$ as well as the loss of satellite feature of Cu 3s due to reduction of Cu^{2+} into Cu^{1+} upon heating to 200 °C.

As for the peak in the high binding energy range, which is persistent from 200 to 300 °C with only a minor shift in binding energy, it is speculated to arise from phosphorus oxide species with one methoxy or methyl group. The fact that the peak at 200 °C seems broader than the one at room temperature indicates the coexistence of multiple similar surface-bound species at 200 °C. Since these surface species are likely to have binding energies very close to each other, it is impossible to differentiate them from each other via peak fitting process. It has been reported that accumulation of a phosphate layer with a stoichiometry similar to P_2O_5 occurs after the removal of all carbonaceous species via annealing of polycrystalline Cu_2O.[33] Considering the TPD results, which have shown that all carbonaceous products evolve in the temperature range of 120 to 320 °C, the peak for 400 °C, which is located at around 134 eV, is assigned as PO_x.

Insight into the Reaction Mechanism from TPD Experiments. Stepwise elimination of methoxy and methyl groups has been reported to be a common feature in the DMMP decomposition pathway.[2] It is usually the case that these groups leave the surface in the gas phase as, for example, methanol, formaldehyde, methane, and/or dimethyl ether.[26,31,38,51,52] In this work, methanol, formaldehyde, and methane are all identified as gaseous products upon heating for both Cu_{100} and $(CuO)_{80}$. The frozen matrix of DMMP sublimes from HOPG at −110 °C, and the monolayer desorbs at around −50 °C (Figure S2). Background TPD experiments and the Cu/P ratio calculated from XPS spectra both indicate that there is no obvious phosphorus-containing species desorbed from the clusters. More details are addressed in the Supporting Information.

In the low temperature region for Cu_{100}, the coincidence of methanol and formaldehyde at around 180 °C is attributed to the disproportionation reaction of surface methoxy (Figure 4a). The low temperature shoulder feature for methanol suggests that the methoxy groups tend to desorb as methanol by reacting with surface hydroxyls before the disproportionation reaction becomes a competitive pathway. Unlike Cu_{100}, $(CuO)_{80}$ has no obvious peak in the low temperature region. Instead, both methanol and formaldehyde have broad rising features, which are likely due to the convolution of multiple desorption peaks. It is known that lattice oxygen in CuO can be activated to oxidize surface adsorbates such as methanol into formaldehyde.[53] In this study, it is shown that the Cu^{2+} moieties within $(CuO)_{80}$ are reduced to Cu^{1+} upon heating to 200 °C. During this process, the lattice oxygen can also be

https://doi.org/10.1021/acs.jpcc.1c00952
J. Phys. Chem. C 2021, 125, 11348−11358

involved in the oxidation of adsorbed methoxy groups. Considering the multiple reaction pathways as well as the drastic changes in structure and composition of the $(CuO)_{80}$ clusters, it is reasonable to expect some broad rising features for methanol and formaldehyde in the TPD spectrum for$(CuO)_{80}$.

In the high temperature region, both Cu_{100} and $(CuO)_{80}$ have discernible peaks for methane and formaldehyde. It is speculated that methane and formaldehyde evolve from further decomposition of MMP instead of adsorbed surface methoxy. In order to obtain more evidence to support this claim, a set of methanol TPD experiments were performed. Methanol, which is known to undergo dissociative adsorption on a variety of metal oxides to form surface methoxy intermediates, has been successfully employed as a "smart" surface probe to quantify surface active sites.[53] In this study, methanol is used as a probe by forming surface methoxy, which should also exist when DMMP decomposes into MMP. As is shown in Figure S4, there is no obvious peak for methane, which indicates that surface methoxy cannot evolve into methane under the experimental conditions in this study. Moreover, methanol has a strong desorption peak at around 50 °C for both Cu_{100} and $(CuO)_{80}$, suggesting an undissociated adsorption form for most of the detected methanol. It should be noted that the methanol peak for Cu_{100} is much broader with a long tail extending above 100 °C. This can be reasonably explained by a reversibly dissociative adsorption form, through which the methanol should desorb at a relatively higher temperature compared to the undissociated adsorption form. This reversibly dissociative adsorption form may also exist on $(CuO)_{80}$; however, the oxidation of surface methoxy can be a competing reaction pathway. As a result, formaldehyde evolves at around 80 °C, and the signal from methanol decreases drastically after peaking at 50 °C. The lattice oxygen within $(CuO)_{80}$ is believed to participate in the formation of formaldehyde, while the lack of lattice oxygen makes Cu_{100} almost inert toward methanol. These results generally agree with the single crystal studies in the literature.[54−57]

Proposed Reaction Scheme Based on XPS and TPD Results. Combined XPS and TPD is a powerful approach to study the decomposition processes of organic molecules on size-selected clusters of interest. TPD can offer evidence on the evolution of gaseous products during the temperature ramping, while XPS acquired after heating the sample to several critical temperatures can elucidate residual species on the surface. Our group has successfully applied this method to shed light on the decomposition mechanism of several organic molecules, including DMMP, on size-selected metal and metal oxide clusters.[31,43] Similarly, the decomposition process of DMMP on Cu_{100} and $(CuO)_{80}$ clusters has been analyzed and compared via combined XPS and TPD in this study. As is shown in Scheme 1, a plausible DMMP decomposition scheme is presented with all the surface species and gaseous products described in the previous sections. Several important interpretations which can be mutually rationalized by both the XPS and TPD results are discussed as well.

First, insights obtained from the XPS results can explain why methanol has a different leading edge but a comparable signal intensity between Cu_{100} and $(CuO)_{80}$ in the low temperature region of the TPD spectra. Specifically, the room temperature XPS shows that the major phosphorus-containing species on Cu_{100} is atomic phosphorus, from which no gaseous product can evolve during a TPD ramp. The weak XPS peak for MMP indicates a small amount of surface methoxy groups on Cu_{100} at room temperature. By contrast, $(CuO)_{80}$ has surface-bound MMP almost exclusively, indicating a fair amount of surface methoxy groups at room temperature. Therefore, the difference in the initial amounts of surface methoxy groups between Cu_{100} and $(CuO)_{80}$ explains why $(CuO)_{80}$ has a stronger rising shoulder feature for methanol in the low temperature region compared to that of Cu_{100}, as is shown in Figure 4. Moreover, considering that the decomposition of both phosphinate and MMP may contribute to the formation of PO_x after heating to 200 °C, it is reasonable to speculate that the decomposition of these two surface species may contribute to the methanol and formaldehyde formation in the low temperature region for Cu_{100}. This also helps to explain why the signal intensity of methanol and formaldehyde for Cu_{100} in the low temperature region is comparable to that of $(CuO)_{80}$, despite the fact that Cu_{100} should have much less surface methoxy groups to begin with at room temperature.

Moreover, the differences in C 1s XPS between Cu_{100} and $(CuO)_{80}$ agree with the fact that the overall TPD signal intensity for $(CuO)_{80}$ is stronger than Cu_{100}. As is shown in Figure S3, for $(CuO)_{80}$, the obvious shoulder feature in the range of 286−287 eV is a strong indication for methoxy groups. The shoulder feature decreases with incremented temperatures, suggesting that those methoxy groups may evolve into gaseous products and leave the surface. By contrast, neither the shoulder feature nor its decreasing process is obviously discernible for Cu_{100}. It has been reported that the C 1s for the methoxy group within MMP is largely indistinguishable from that of methoxy groups absorbed on CuO;[32] however, the methoxy group on clean Cu(110) may have a slightly lower C 1s binding energy.[56] Therefore, the C 1s XPS spectra not only provide additional evidence for the abundance of methoxy groups on $(CuO)_{80}$, but also agrees with the fact that $(CuO)_{80}$ has stronger RGA signals for methoxy-originated gaseous products, such as methanol and formaldehyde.

Furthermore, broad peaks are expected in both XPS and TPD spectra based on fundamental considerations. Theoretical studies have shown that dynamic fluxionality can cause supported clusters to populate many distinct structural and stoichiometric states under reaction conditions.[58] Hence, the reaction interface should be viewed as an evolving statistical ensemble of many structures.[59] This theory has been exemplified by size-selected cluster catalysis experiments, in which the size-dependent properties are explained by different compositions of thermal ensembles.[60,61] In this study, it is believed that the support (HOPG) and the absorbate (DMMP) can affect the structure of the clusters, causing the ensembles to change for all reaction intermediates. The structural dynamics can become even more complex during the heating process, when reaction intermediates can follow different reaction pathways and the lattice oxygen within $(CuO)_{80}$ is activated. Since both XPS and TPD can only provide the ensemble-average information, it is reasonable to expect that the XPS peaks are broader at elevated temperatures and that the TPD peaks are more broadened for $(CuO)_{80}$ in the low temperature region.

Although all of the above discussion shows that our overall reaction scheme is reasonable considering the mutual agreement between the XPS and TPD results, it should be realized that the XPS results cannot be directly mapped to the TPD results. The reason is that TPD is the result of continuous measurements during a programmed linear temperature ramp,

https://doi.org/10.1021/acs.jpcc.1c00952
J. Phys. Chem. C 2021, 125, 11348−11358

while XPS is taken at room temperature, which is a relatively thermodynamically stable state reached after prolonged heating of the sample at certain critical temperatures. The P 2p XPS does show well-separated peaks for certain surface species, especially for atomic phosphorus on Cu_{100}. However, the presence of broad peaks and low signal-to-noise ratio in the heating data makes it very hard to conclusively assign peaks. Moreover, the unresolved peaks in the TPD data also make it difficult to relate every surface species to their corresponding gaseous products. Additional characterizations, such as FT-IR, isotopic labeling, and computational work would further validate more details in the proposed reaction scheme; however, these efforts are outside the scope of the study presented here.

CONCLUSIONS

In this work, we use combined XPS and TPD to investigate the room temperature decomposition and thermal decomposition of DMMP on size selected Cu_{100} and $(CuO)_{80}$ clusters supported on HOPG. Cu_{100} has shown remarkable reactivities toward DMMP, which is drastically different from $(CuO)_{80}$. At room temperature, the XPS results show that most of the adsorbed DMMP molecules decompose completely into atomic phosphorus on Cu_{100}, while phosphine, phosphinate, and phosphonate groups may exist in only small amounts. By contrast, DMMP mainly dissociates into surface-bound MMP and methoxy species through P−OCH_3 bond scission on $(CuO)_{80}$ at room temperature, which is commonly seen on many other metal oxides. TPD results show evidence of two distinct desorption regions and that methanol, formaldehyde, and methane are the three main volatile products for both Cu_{100} and $(CuO)_{80}$. The differences between the TPD results can be correlated to the XPS results to some degree. A set of methanol-probed TPD experiments, which show the desorption of formaldehyde from $(CuO)_{80}$ but not from Cu_{100} and no methane production for either cluster, suggest that lattice oxygen within $(CuO)_{80}$ is involved in thermal decomposition of DMMP and that methane originates from the methyl group within DMMP instead of the surface methoxy species.

This work highlights a unique method to synthesize small clusters and analyze their reactivities toward DMMP. The mass-selected soft-landing deposition method makes it efficient to prepare small copper and cupric oxide clusters of desired size on a prepared surface. Combined XPS and TPD offers a powerful approach to analyze the decomposition process of DMMP. The results not only add to the library of metal and metal oxide clusters studied for degradation of CWA simulants but also showcase how changing the metal oxidation states can affect the reactivity toward DMMP substantially. It should be emphasized that the remarkable reactivities of Cu_{100} toward DMMP at room temperature should motivate more work on metallic copper materials. Besides oxidative decomposition of CWAs, for which many metal oxide materials have been explored, reductive decomposition, which is exemplified by Cu_{100} in this work, may be another promising path.

ASSOCIATED CONTENT

Supporting Information

The Supporting Information is available free of charge at https://pubs.acs.org/doi/10.1021/acs.jpcc.1c00952.

XPS for molecular DMMP, TPD spectrum on DMMP physi-desorption, XPS for C 1s, explanations for fragmentation correction and background subtraction, and P/Cu ratio change based on quantitative analysis for XPS spectra and methanol-probed TPD (PDF)

AUTHOR INFORMATION

Corresponding Author

Kit H. Bowen − *Department of Chemistry, Johns Hopkins University, Baltimore, Maryland 21218, United States;* orcid.org/0000-0002-2858-6352; Email: kbowen@jhu.edu

Authors

Linjie Wang − *Department of Chemistry, Johns Hopkins University, Baltimore, Maryland 21218, United States;* orcid.org/0000-0002-6558-1753

Michael Denchy − *Department of Chemistry, Johns Hopkins University, Baltimore, Maryland 21218, United States*

Nicolas Blando − *Department of Chemistry, Johns Hopkins University, Baltimore, Maryland 21218, United States*

Lucas Hansen − *Department of Chemistry, Johns Hopkins University, Baltimore, Maryland 21218, United States*

Ben Bilik − *Department of Chemistry, Johns Hopkins University, Baltimore, Maryland 21218, United States*

Xin Tang − *Department of Chemistry, Johns Hopkins University, Baltimore, Maryland 21218, United States*

Zachary Hicks − *Department of Chemistry, Johns Hopkins University, Baltimore, Maryland 21218, United States*

Complete contact information is available at: https://pubs.acs.org/10.1021/acs.jpcc.1c00952

Notes

The authors declare no competing financial interest.

ACKNOWLEDGMENTS

This material is based upon work supported by the Defense Threat Reduction Agency (DTRA) under Grant Number HDTRA11510005 and the Army Research Office (ARO) under Grant Number W911NF2020207.

REFERENCES

(1) McGrath, J. W.; Chin, J. P.; Quinn, J. P. Organophosphonates revealed: new insights into the microbial metabolism of ancient molecules. *Nat. Rev. Microbiol.* **2013**, *11*, 412−419.

(2) Kim, K.; Tsay, O. G.; Atwood, D. A.; Churchill, D. G. Destruction and detection of chemical warfare agents. *Chem. Rev.* **2011**, *111*, 5345−5403.

(3) Li, Y. X.; Klabunde, K. J. Nano-scale metal oxide particles as chemical reagents. Destructive adsorption of a chemical agent simulant, dimethyl methylphosphonate, on heat-treated magnesium oxide. *Langmuir* **1991**, *7*, 1388−1393.

(4) Ekerdt, J. G.; Klabunde, K. J.; Shapley, J. R.; White, J. M.; Yates, J. T. Surface chemistry of organophosphorus compounds. *J. Phys. Chem.* **1988**, *92*, 6182−6188.

(5) Henych, J.; Janos, P.; Kormunda, M.; Tolasz, J.; Stengl, V. Reactive adsorption of toxic organophosphates parathion methyl and DMMP on nanostructured Ti/Ce oxides and their composites. *Arabian J. Chem.* **2019**, *12*, 4258−4269.

(6) Jaiswal, M.; Chauhan, D.; Sankararamakrishnan, N. Copper chitosan nanocomposite: synthesis, characterization, and application in removal of organophosphorous pesticide from agricultural runoff. *Environ. Sci. Pollut. Res.* **2012**, *19*, 2055−2062.

(7) Kaur, P.; Bansal, P.; Sud, D. Heterostructured nanophotocatalysts for degradation of organophosphate pesticides from aqueous streams. *J. Korean Chem. Soc.* **2013**, *57*, 382−388.

(8) Rani, M.; Shanker, U. Degradation of traditional and new emerging pesticides in water by nanomaterials: recent trends and future recommendations. *Int. J. Environ. Sci. Technol.* **2018**, *15*, 1347−1380.
(9) Mitchell, M. B.; Sheinker, V. N.; Mintz, E. A. Adsorption and decomposition of dimethyl methylphosphonate on metal oxides. *J. Phys. Chem. B* **1997**, *101*, 11192−11203.
(10) Bermudez, V. M. Effect of humidity on the interaction of dimethyl methylphosphonate (DMMP) vapor with SiO_2 and Al_2O_3 surfaces, studied using infrared attenuated total reflection spectroscopy. *Langmuir* **2010**, *26*, 18144−18154.
(11) Templeton, M. K.; Weinberg, W. H. Decomposition of phosphonate esters adsorbed on aluminum oxide. *J. Am. Chem. Soc.* **1985**, *107*, 774−779.
(12) Sheinker, V. N.; Mitchell, M. B. Quantitative study of the decomposition of dimethyl methylphosphonate (DMMP) on metal oxides at room temperature and above. *Chem. Mater.* **2002**, *14*, 1257−1268.
(13) Wilmsmeyer, A. R.; Uzarski, J.; Barrie, P. J.; Morris, J. R. Interactions and binding energies of dimethyl methylphosphonate and dimethyl chlorophosphate with amorphous silica. *Langmuir* **2012**, *28*, 10962−10967.
(14) Kanan, S. M.; Tripp, C. P. An infrared study of adsorbed organophosphonates on silica: a prefiltering strategy for the detection of nerve agents on metal oxide sensors. *Langmuir* **2001**, *17*, 2213−2218.
(15) Taylor, D. E.; Runge, K.; Cory, M. G.; Burns, D. S.; Vasey, J. L.; Hearn, J. D.; Griffith, K.; Henley, M. V. Surface binding of organophosphates on silica: comparing experiment and theory. *J. Phys. Chem. C* **2013**, *117*, 2699−2708.
(16) Aurianblajeni, B.; Boucher, M. M. Interaction of dimethyl methylphosphonate with metal oxides. *Langmuir* **1989**, *5*, 170−174.
(17) Moss, J. A.; Szczepankiewicz, S. H.; Park, E.; Hoffmann, M. R. Adsorption and photodegradation of dimethyl methylphosphonate vapor at TiO_2 surfaces. *J. Phys. Chem. B* **2005**, *109*, 19779−19785.
(18) Trubitsyn, D. A.; Vorontsov, A. V. Experimental study of dimethyl methylphosphonate decomposition over anatase TiO_2. *J. Phys. Chem. B* **2005**, *109*, 21884−21892.
(19) Kim, C. S.; Lad, R. J.; Tripp, C. P. Interaction of organophosphorous compounds with TiO_2 and WO_3 surfaces probed by vibrational spectroscopy. *Sens. Actuators, B* **2001**, *76*, 442−448.
(20) Rusu, C. N.; Yates, J. T. Photooxidation of dimethyl methylphosphonate on TiO_2 powder. *J. Phys. Chem. B* **2000**, *104*, 12299−12305.
(21) Panayotov, D. A.; Morris, J. R. Uptake of a chemical warfare agent simulant (DMMP) on TiO_2: reactive adsorption and active site poisoning. *Langmuir* **2009**, *25*, 3652−3658.
(22) Panayotov, D. A.; Morris, J. R. Thermal decomposition of a chemical warfare agent simulant (DMMP) on TiO_2: adsorbate reactions with lattice oxygen as studied by infrared spectroscopy. *J. Phys. Chem. C* **2009**, *113*, 15684−15691.
(23) Rusu, C. N.; Yates, J. T. Adsorption and decomposition of dimethyl methylphosphonate on TiO_2. *J. Phys. Chem. B* **2000**, *104*, 12292−12298.
(24) Mitchell, M. B.; Sheinker, V. N.; Tesfamichael, A. B.; Gatimu, E. N.; Nunley, M. Decomposition of dimethyl methylphosphonate (DMMP) on supported cerium and iron co-impregnated oxides at room temperature. *J. Phys. Chem. B* **2003**, *107*, 580−586.
(25) Mitchell, M. B.; Sheinker, V. N.; Cox, W. W.; Gatimu, E. N.; Tesfamichael, A. B. The room temperature decomposition mechanism of dimethyl methylphosphonate (DMMP) on alumina-supported cerium oxide - participation of nano-sized cerium oxide domains. *J. Phys. Chem. B* **2004**, *108*, 1634−1645.
(26) Chen, D. A.; Ratliff, J. S.; Hu, X. F.; Gordon, W. O.; Senanayake, S. D.; Mullins, D. R. Dimethyl methylphosphonate decomposition on fully oxidized and partially reduced ceria thin films. *Surf. Sci.* **2010**, *604*, 574−587.
(27) Tang, X.; Hicks, Z.; Gantefor, G.; Eichhorn, B. W.; Bowen, K. H. Adsorption and decomposition of DMMP on size-selected $(WO_3)_3$ clusters. *Chemistry Select* **2018**, *3*, 3718−3721.
(28) Head, A. R.; Tsyshevsky, R.; Trotochaud, L.; Yu, Y.; Karslioglu, O.; Eichhorn, B.; Kuklja, M. M.; Bluhm, H. Dimethyl methylphosphonate adsorption and decomposition on MoO_2 as studied by ambient pressure x-ray photoelectron spectroscopy and DFT calculations. *J. Phys.: Condens. Matter* **2018**, *30*, 134005.
(29) Head, A. R.; Tsyshevsky, R.; Trotochaud, L.; Yu, Y.; Kyhl, L.; Karslioglu, O.; Kuklja, M. M.; Bluhm, H. Adsorption of dimethyl methylphosphonate on MoO_3: the role of oxygen vacancies. *J. Phys. Chem. C* **2016**, *120*, 29077−29088.
(30) Head, A. R.; Tang, X.; Hicks, Z.; Wang, L. J.; Bleuel, H.; Holdren, S.; Trotochaud, L.; Yu, Y.; Kyhl, L.; Karslioglu, O.; et al. Thermal desorption of dimethyl methylphosphonate from MoO_3. *Catal. Struct. React.* **2017**, *3*, 112−118.
(31) Tang, X.; Hicks, Z.; Wang, L. J.; Gantefor, G.; Bowen, K. H.; Tsyshevsky, R.; Sun, J. W.; Kuklja, M. M. Adsorption and decomposition of dimethyl methylphosphonate on size-selected $(MoO_3)_3$ clusters. *Phys. Chem. Chem. Phys.* **2018**, *20*, 4840−4850.
(32) Trotochaud, L.; Tsyshevsky, R.; Holdren, S.; Fears, K.; Head, A. R.; Yu, Y.; Karslioglu, O.; Pletincx, S.; Eichhorn, B.; Owrutsky, J.; et al. Spectroscopic and computational investigation of room-temperature decomposition of a chemical warfare agent simulant on polycrystalline cupric oxide. *Chem. Mater.* **2017**, *29*, 7483−7496.
(33) Trotochaud, L.; Head, A. R.; Buchner, C.; Yu, Y.; Karslioglu, O.; Tsyshevsky, R.; Holdren, S.; Eichhorn, B.; Kuklja, M. M.; Bluhm, H. Room temperature decomposition of dimethyl methylphosphonate on cuprous oxide yields atomic phosphorus. *Surf. Sci.* **2019**, *680*, 75−87.
(34) Guo, X.; Yoshinobu, J.; Yates, J. T. Decomposition of an organophosphonate compound (dimethyl methylphosphonate) on the Ni(111) and Pd(111) surfaces. *J. Phys. Chem.* **1990**, *94*, 6839−6842.
(35) Henderson, M. A.; White, J. M. Adsorption and decomposition of dimethyl methylphosphonate on Pt(111). *J. Am. Chem. Soc.* **1988**, *110*, 6939−6947.
(36) Hegde, R. I.; Greenlief, C. M.; White, J. M. Surface chemistry of dimethyl methylphosphonate on Rh(100). *J. Phys. Chem.* **1985**, *89*, 2886−2891.
(37) Smentkowski, V. S.; Hagans, P.; Yates, J. T. Study of the catalytic destruction of dimethyl methylphosphonate: oxidation over Mo(110). *J. Phys. Chem.* **1988**, *92*, 6351−6357.
(38) Ma, S.; Zhou, J.; Kang, Y. C.; Reddic, J. E.; Chen, D. A. Dimethyl methylphosphonate decomposition on Cu surfaces: supported Cu nanoclusters and films on TiO_2(110). *Langmuir* **2004**, *20*, 9686−9694.
(39) McEntee, M.; Gordon, W. O.; Balboa, A.; Delia, D. J.; Pitman, C. L.; Pennington, A. M.; Rolison, D. R.; Pietron, J. J.; DeSario, P. A. Mesoporous copper nanoparticle/TiO_2 aerogels for room-temperature hydrolytic decomposition of the chemical warfare simulant dimethyl methylphosphonate. *ACS Appl. Nano Materials* **2020**, *3*, 3503−3512.
(40) Vajda, S.; White, M. G. Catalysis applications of size-selected cluster deposition. *ACS Catal.* **2015**, *5*, 7152−7176.
(41) Ford, T. A. Matrix isolation infrared spectroscopy - Comparison of theory with experiment. *Can. J. Anal. Sci. Spectrosc.* **1998**, *43*, 113−121.
(42) Li, Z. J.; Fang, Z. T.; Kelley, M. S.; Kay, B. D.; Rousseau, R.; Dohnalek, Z.; Dixon, D. A. Ethanol conversion on cyclic $(MO_3)_3$ (M = Mo, W) clusters. *J. Phys. Chem. C* **2014**, *118*, 4869−4877.
(43) Wang, L. J.; Blando, N.; Hicks, Z.; Denchy, M.; Tang, X.; Bleuel, H.; Zhang, M. S.; Gantefor, G.; Bowen, K. H. Combined TPD and XPS study of ligation and decomposition of 1,6-hexanedithiol on size-selected copper clusters supported on HOPG. *J. Phys. Chem. C* **2018**, *122*, 2173−2183.
(44) Schmieg, S. J.; Belton, D. N. Highly oriented pyrolytic graphite by XPS. *Surf. Sci. Spectra* **1992**, *1*, 333−336.

https://doi.org/10.1021/acs.jpcc.1c00952
J. Phys. Chem. C 2021, 125, 11348−11358

(45) Tang, X.; Li, X.; Wang, Y.; Wepasnick, K.; Lim, A.; Fairbrother, D. H.; Bowen, K. H.; Mangler, T.; Noessner, S.; Wolke, C.; et al. Size selected clusters on surfaces. *J. Phys.: Conf. Ser.* **2013**, *438*, 012005.
(46) Moulder, J. F. S. W. F.; Sobol, P. E.; Bomben, K. D. *Handbook of x-ray photoelectron spectroscopy*, Chastain, J., Ed.; Perkin-Elmer Corporation: Eden Prairie, MN. 1992.
(47) Lai, Y. H.; Yeh, C. T.; Lin, H. J.; Chen, C. T.; Hung, W. H. Thermal reaction of trimethylphosphine and triethylphosphine on Cu(110). *J. Phys. Chem. B* **2002**, *106*, 1722−1727.
(48) Gu, Z.; Hohn, K. L. Catalytic oxidation of methanol on nanoscale copper oxide and nickel oxide. *Ind. Eng. Chem. Res.* **2004**, *43*, 30−35.
(49) Zhou, L.; Gunther, S.; Moszynski, D.; Imbihl, R. Reactivity of oxidized copper surfaces in methanol oxidation. *J. Catal.* **2005**, *235*, 359−367.
(50) Wang, Y. W.; Im, J. S.; Soares, J. W.; Steeves, D. M.; Whitten, J. E. Thiol adsorption on and reduction of copper oxide particles and surfaces. *Langmuir* **2016**, *32*, 3848−3857.
(51) Zhou, J.; Ma, S.; Kang, Y. C.; Chen, D. A. Dimethyl methylphosphonate decomposition on titania-supported Ni clusters and films: a comparison of chemical activity on different Ni surfaces. *J. Phys. Chem. B* **2004**, *108*, 11633−11644.
(52) Ratliff, J. S.; Tenney, S. A.; Hu, X. F.; Conner, S. F.; Ma, S. G.; Chen, D. A. Decomposition of dimethyl methylphosphonate on Pt, Au, and Au-Pt Clusters supported on TiO_2(110). *Langmuir* **2009**, *25*, 216−225.
(53) Badlani, M.; Wachs, I. E. Methanol: a "smart" chemical probe molecule. *Catal. Lett.* **2001**, *75*, 137−149.
(54) Russell, J. N.; Gates, S. M.; Yates, J. T. Reaction of methanol with Cu(111) and Cu(111) + O(Ads). *Surf. Sci.* **1985**, *163*, 516−540.
(55) Ryberg, R. The Oxidation of methanol on Cu(100). *J. Chem. Phys.* **1985**, *82*, 567−573.
(56) Ammon, C.; Bayer, A.; Held, G.; Richter, B.; Schmidt, T.; Steinruck, H. P. Dissociation and oxidation of methanol on Cu(110). *Surf. Sci.* **2002**, *507*, 845−850.
(57) Sakong, S.; Sendner, C.; Gross, A. Partial oxidation of methanol on Cu(110): energetics and kinetics. *J. Mol. Struct.: THEOCHEM* **2006**, *771*, 117−122.
(58) Zandkarimi, B.; Alexandrova, A. N. Surface-supported cluster catalysis: ensembles of metastable states run the show. *Wiley Interdiscip. Rev.: Comput. Mol. Sci.* **2019**, *9*, No. e1420.
(59) Zhang, Z. S.; Zandkarimi, B.; Alexandrova, A. N. Ensembles of metastable states govern heterogeneous catalysis on dynamic interfaces. *Acc. Chem. Res.* **2020**, *53*, 447−458.
(60) Baxter, E. T.; Ha, M. A.; Cass, A. C.; Alexandrova, A. N.; Anderson, S. L. Ethylene dehydrogenation on Pt_4, Pt_7, Pt_8 clusters on Al_2O_3: strong cluster size dependence linked to preferred catalyst morphologies. *ACS Catal.* **2017**, *7*, 3322−3335.
(61) Ha, M. A.; Baxter, E. T.; Cass, A. C.; Anderson, S. L.; Alexandrova, A. N. Boron switch for selectivity of catalytic dehydrogenation on size-selected Pt clusters on Al_2O_3. *J. Am. Chem. Soc.* **2017**, *139*, 11568−11575.

https://doi.org/10.1021/acs.jpcc.1c00952
J. Phys. Chem. C 2021, 125, 11348−11358